Springer

KSME

Journal of Mechanical Science and Technology 28 (4) (2014) 1297~1310
www.springerlink.com/content/1738-494x
DOI 10.1007/s12206-014-0119-1

Numerical study of blowing and suction slot geometry optimization on NACA 0012 airfoil †

Kianoosh Yousefi*, Reza Saleh and Peyman Zahedi

Department of Mechanical Engineering, College of Engineering, Mashhad Branch, Islamic Azad University, Mashhad, Iran

(Manuscript Received March 1, 2013; Revised July 10, 2013; Accepted November 9, 2013)

Abstract

The effects of jet width on blowing and suction flow control were evaluated for a NACA 0012 airfoil. RANS equations were employed in conjunction with a Menter's shear stress turbulent model. Tangential and perpendicular blowing at the trailing edge and perpendicular suction at the leading edge were applied on the airfoil upper surface. The jet widths were varied from 1.5% to 4% of the chord length, and the jet velocity was 0.3 and 0.5 of the free-stream velocity. Results of this study demonstrated that when the blowing jet width increases, the lift-to-drag ratio rises continuously in tangential blowing and decreases quasi-linearly in perpendicular blowing. The jet widths of 3.5% and 4% of the chord length are the most effective amounts for tangential blowing, and smaller jet widths are more effective for perpendicular blowing. The lift-to-drag ratio improves when the suction jet width increases and reaches its maximum value at 2.5% of the chord length.

Keywords: Flow control; Jet width; Lift and drag coefficients; Slot geometry optimization; Suction; Blowing

1. Introduction

Although potential theory can be used to explain many aerodynamic phenomena, the boundary layer significantly alters theoretical predictions in some cases. An example of which is the flow passing an airfoil. At low angles of attack, the streamline pattern with such a shape is closed to the predictions of inviscid theory. However, a drag force unaccounted for by such a theory exists. This drag is large because of viscous shear forces and is called skin-friction drag. In the regions over the surface, where the boundary layer flow is laminar, the fluid mixing and viscous skin friction are low. However, such laminar flows are often unstable and develop into turbulent flows. Turbulent flows involve more rapid mixing than laminar flows, which produce higher skin-friction drag. The combined action of viscous forces and an adverse pressure gradient produces a reverse of the flow next to the surface, which causes separation of the adjacent flow from the surface. The presence of the boundary layer has produced many design problems in all areas of fluid mechanics. The most intensive investigations have been directed toward its effect on the lift and drag of wings. Techniques developed to manipulate the boundary layer, either to increase the lift or decrease the drag, are classified under the general heading of boundary layer control or flow control [1]. In 1961, Flatt indicated that boundary layer control includes any mechanism or process which the boundary layer of a fluid flow is caused to behave differently than it normally would when the flow develops naturally along a smooth straight surface. Methods of flow control to achieve transition delay, separation postponement, lift enhancement, drag reduction, turbulence augmentation, and noise suppression have been considered [2].

Numerous studies have been conducted on flow control techniques. Prandtl [3] was the first scientist who employed boundary layer suction on a cylindrical surface to delay boundary layer separation in 1904. The earliest known experimental works [4-6] on boundary layer suction for wings, primarily in the wind tunnel, were conducted in the late 1930s and the 1940s. Suction and blowing approaches have emerged and have been studied in a variety of experiments [7-11]. Such experiments have demonstrated that suction and blowing can modify the pressure distribution over an airfoil surface and have a substantial effect on lift and drag coefficients. Over the past few decades, various numerical works have been performed on the most common NACA airfoils to measure the lift and drag coefficients under different flow conditions [12-16]. In these studies, the effects of zero net mass flux oscillatory jet (synthetic jet) and leading edge blowing/suction were considered on the vortex flow passing airfoils. Moreover, flow control methods, such as suction, blowing, and synthetic jets, have been investigated through analytical methods [17-19]

*Corresponding author. Tel.: +98 9121715219, Fax.: +98 2177923881
E-mail address: kianoosh_py@yahoo.com
† Recommended by Associate Editor Yang Na

over thick and NACA airfoils.

Huang et al. [20] studied the suction and blowing flow control techniques on a NACA 0012 airfoil. When jet location and angle of attack were combined, perpendicular suction at the leading edge increased lift coefficient better than other suction situations. The tangential blowing at downstream locations was found to lead to the maximum increase in the lift coefficient value. Rosas [21] numerically investigated flow separation control through oscillatory fluid injection, in which lift coefficient dramatically increased. Beliganur and Raymond [22] applied an evolutionary algorithm to optimize flow control. Results of their study showed that the use of two suction jets along with two blowing jets enhanced the lift-to-drag ratio for a NACA 0012 airfoil. Akcayoz and Tuncer [23] examined the optimization of synthetic jet parameters on a NACA 0015 airfoil in different angles of attack to maximize the lift-to-drag ratio. Their results revealed that the optimum jet location moved toward the leading edge and the optimum jet angle incremented as the angle of attack increased. Jensch et al. [24] numerically conducted an aerodynamic analysis of a two-dimensional airfoil to improve the efficiency of a circulation control system. Varied slot heights at different flap deflection angles and leading edge blowing were investigated to optimize high-lift performance. The occurrence of a thin separation bubble near the leading edge was prevented through applying a second blowing slot at the leading edge.

With the development of computational facilities in recent years, computational fluid dynamics (CFD) has been increasingly used to investigate boundary layer control. Numerous flow control studies through CFD approaches [25-33] have been conducted to investigate the effects of blowing, suction, and synthetic jets on the aerodynamic characteristics of airfoils. In the current study, the optimization of blowing and suction slot geometries, including suction and blowing jet widths, is numerically analyzed. Nearly 500 numerical simulations are performed with several parameters, such as jet amplitude, jet width, jet angle, and jet momentum coefficient at different angles of attack, on a NACA 0012 airfoil.

2. Governing equations

The fluid flow was modeled as a two-dimensional, unsteady, turbulent, and viscous incompressible flow with constant properties. The governing partial differential equations for mass and momentum conservation are as follows:

$$\frac{\partial \bar{u}_i}{\partial x_i}=0, \tag{1}$$

$$\frac{\partial}{\partial x_j}\left(\bar{u}_i\bar{u}_j\right)=-\frac{1}{\rho}\frac{\partial \bar{P}}{\partial x_i}+\frac{\partial}{\partial x_j}\left[\nu\frac{\partial \bar{u}_i}{\partial x_j}-\overline{u_i'u_j'}\right] \tag{2}$$

where ρ is the density, $\bar{P}$ is the mean pressure, ν is the kinematic viscosity, and $\bar{u}$ is the mean velocity. The term $-\overline{u_i'u_j'}$ is the Reynolds stress tensor that incorporates the effects of turbulent fluctuations. The Reynolds stresses were modeled via the Boussinesq approximation [34], in which the deviatoric part is considered proportional to the strain rate tensor through the turbulent viscosity. The incompressible form of the Boussinesq approximation is

$$\overline{u_i'u_j'}=\nu_t\left(\frac{\partial \bar{u}_i}{\partial x_j}+\frac{\partial \bar{u}_j}{\partial x_i}\right)-\frac{2}{3}k\delta_{ij} \tag{3}$$

$$k=\frac{1}{2}\left(\overline{u'^2}+\overline{v'^2}+\overline{w'^2}\right) \tag{4}$$

where ν_t is the turbulent viscosity, k is the average kinetic energy of the velocity fluctuations, and δ_{ij} is the Kronecker delta. To simulate the turbulent flow, eddy or turbulent viscosity distribution was employed rather than the Reynolds stress tensor through eddy viscosity turbulent models, including algebraic or zero-equation models, one-equation models, and two-equation models.

The turbulence model used in the present computation was the Menter's shear stress transport two-equation model (k-ω SST), which provides excellent predictive capability for flows with separation. This model includes k-ω and k-ε standard models, which improve the calculations of boundary layer flows with separation and remove the sensitivity of k-ω model in external flows. The transport equations in the Menter's shear stress model are as follows:

$$\frac{\partial}{\partial x_i}(\rho U_i k)=\tilde{P}_k-\beta^*\rho k\omega+\frac{\partial}{\partial x_i}\left[\left(\mu+\sigma_k\mu_t\right)\frac{\partial k}{\partial x_i}\right] \tag{5}$$

$$\frac{\partial}{\partial x_i}(\rho U_i \omega)=\alpha\rho S^2-\beta\rho\omega^2+\frac{\partial}{\partial x_i}\left[\left(\mu+\sigma_\omega\mu_t\right)\frac{\partial \omega}{\partial x_i}\right]+2\left(1-F_1\right)\rho\sigma_{w2}\frac{1}{\omega}\frac{\partial k}{\partial x_i}\frac{\partial \omega}{\partial x_i} \tag{6}$$

where F_1 is the blending function, S is the invariant measure of the strain rate, β^* is 0.09, and σ_{w2} is 0.856. The blending function is equal to zero when is away from the surface (k-ε model) and switches over to unity inside the boundary layer (k-ω model). A production limiter, $\tilde{P}_k$, was used in the SST model to prevent the build-up of turbulence in the stagnation regions. All constants were computed by a blend from the corresponding constant of the k-ε and k-ω models via α, σ_k, σ_ω, and so on [35].

3. Numerical simulation

3.1 Parameter selection

The commercial RANS-based code FLUENT, which follows a finite volume computational procedure, was used in this study. The first- and second-order upwind schemes were employed to discretize the convective terms in the momentum and turbulence equations. The central difference scheme was also used for the diffusive terms, and SIMPLE algorithm was applied for pressure–velocity coupling.

Calculations were performed over the NACA 0012 airfoil with 1 m chord length and a chord Reynolds number of 5×10^5. The NACA 0012 profile, blowing and suction jet location (L_j), blowing and suction angle (θ), and jet width (h) are

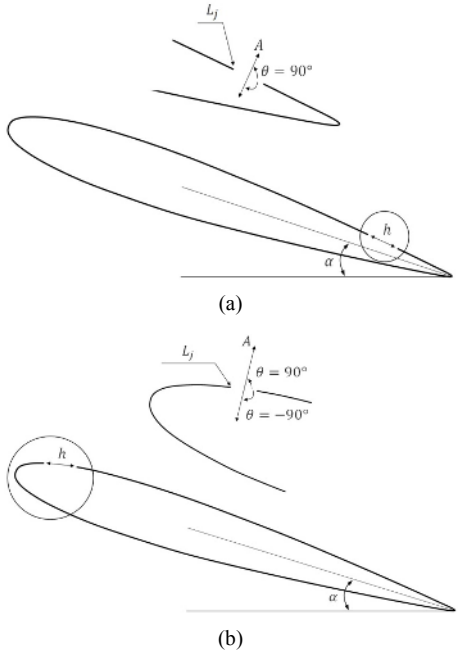

Fig. 1. NACA 0012 airfoil with blowing and suction slots: (a) blowing slot; (b) suction slot.

shown in Fig. 1. A previous study [20], under similar conditions at Re = 5×10^5 and jet width of 2.5% of the chord length, has shown that the blowing at downstream locations, approximately 0.4 and 0.8, is better than other blowing situations for increasing lift. Moreover, recent investigations [21 and 23] have indicated that blowing at the trailing edge is more appropriate in various flow conditions than that at other locations. Therefore, the blowing slot was considered at 80% of the chord length from the leading edge in this work.

Meanwhile, suction at the leading edge, approximately 10% of the chord length, is better than other positions in improving the lift-to-drag ratio at different flow conditions over different airfoils [20, 21, 23, 25]. In this study, the suction slot was therefore located at 10% of the chord length from the leading edge. The blowing and suction slot widths were varied from 1.5% to 4% of the chord length, and the jet amplitude (the jet velocity-to-free-stream velocity ratio) was 0.3 and 0.5. The angles of attack analyzed were 12, 14, 16, and 18°. The jet amplitude and jet entrance velocity are defined as follows:

$$A = \frac{u_j}{u_\infty} \tag{7}$$

$$u = A.\cos(\theta+\beta) \tag{8}$$

$$v = A.\sin(\theta+\beta) \tag{9}$$

where β is the angle between the free-stream velocity direction and the local jet surface, and θ is the angle between the local jet surface and the jet output velocity direction. Negative θ represents suction condition, and positive θ indicates blowing condition. For tangential blowing, perpendicular blowing, and perpendicular suction, θ is +90°, 0°, and −90°, respectively.

Finally, the jet momentum coefficient is as follows:

$$C_\mu = \frac{\rho.h.v_j^2}{\rho.C.u_\infty^2} = \frac{h}{C} \times \frac{u_j^2}{u_\infty^2} \tag{10}$$

$$H = \frac{h}{C} \tag{11}$$

$$C_\mu = H.A^2. \tag{12}$$

Eq. (12) indicates that the jet momentum coefficient depends on two non-dimensional factors, namely, jet amplitude (A) and dimensionless jet width (H). A moving fluid exerts pressure and shear forces on the body surface. Both of these forces generally have components in the normal and tangential directions of flow; thus, the drag force is due to the combined effects of pressure (pressure drag) and wall shear forces (viscous drag) in the flow direction. Pressure and wall shear forces occur in the normal direction, and their sum (pressure lift and viscous lift) is called lift. The lift and drag forces are expressed as follows:

$$F_D = \int dF_x = \int P.\cos\theta\ dA + \int \tau_w.\sin\theta\ dA \tag{13}$$

$$F_L = \int dF_y = -\int P.\sin\theta\ dA + \int \tau_w.\cos\theta\ dA. \tag{14}$$

Dimensionless numbers of drag and lift coefficients, which represent the drag and lift characteristics of the body, are more convenient to use than other numbers. They are defined as follows:

$$C_D = C_{D,P} + C_{D,V} = \frac{F_D}{\frac{1}{2}\rho V^2 A} \tag{15}$$

$$C_L = C_{L,P} + C_{L,V} = \frac{F_L}{\frac{1}{2}\rho V^2 A} \tag{16}$$

where the subscripts P and V refer to pressure and viscous, respectively. In the calculations of airfoils, A is taken to be the planform area. The pressure and viscous drag and the pressure and viscous lift were considered in all current simulations.

3.2 Numerical solution method

The first- and second-order upwind methods were employed to discretize the governing equations. In the simulations, first-order upwind discretization in space was used, and then, the resulting system of equations was solved through SIMPLE procedure until a convergence criteria of O(5) reduction in all dependent residuals was satisfied. The second-order upwind method was then applied to discretize the equations. The equations were resolved through SIMPLE method until a precise convergence was achieved at O(7) in all dependent residuals. The results obtained from the first-order upwind method were used as an initial assumption for the second-order upwind method.

A C-type-structured grid with multizonal blocks, which is shown in Fig. 2, was generated as computational area. The computational area was large enough to prevent the outer

Table 1. Grid independence study for NACA 0012 airfoil at a Reynolds number of 5×10^5 and an angle of attack of 16°.

Number of cells	Angle of attack of 10°		Angle of attack of 16°	
	Lift coefficient	Drag coefficient	Lift coefficient	Drag coefficient
8096	0.82201	0.07858	0.64594	0.20889
17160	0.91364	0.05898	1.05134	0.12544
24480	0.90865	0.05525	1.09073	0.11567
40640	0.90873	0.05332	1.12352	0.10938
58080	0.90878	0.05394	1.12319	0.11187

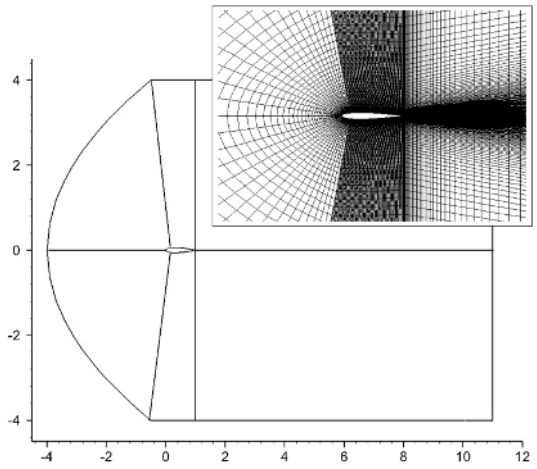

Fig. 2. C-type-structured mesh with multizonal blocks.

boundary from affecting the near flow field around the airfoil. The inlet (left) and lower boundaries were fixed, with a uniform inlet velocity, u_∞ = 7.3 m/s. The upper and outer (right) boundary conditions were free-stream boundaries that satisfy the Neumann condition. Moreover, no-slip boundary condition was used at solid surfaces. A low free-stream turbulence level was used to match the wind tunnel characteristics, such that the stream turbulence intensity was selected as less than 0.1%. Different sized grids were used to ensure grid independence of the calculated results through the study of lift and drag coefficients at angles of attack of 10 and 16° for basic condition, without jets implemented on the airfoil. According to Table 1, the grid size giving a grid independent result with reasonable accuracy was selected to be 40640 cells.

An interval size of 0.005 with 412 nodes was used on the upper and lower surfaces of airfoil, where the first-cell height was 1×10^4. To simulate the boundary layer flow, the first layer grid near the wall satisfied the y-plus between 0.2 and 1.6. The mesh features and y-plus distribution over the airfoil are shown in Table 2 and Fig. 3, respectively. The interval size was reduced to 0.00125 for blowing and suction slots, as indicated in Fig. 4.

The residuals in all simulations were continued until the lift and drag coefficients reach a full convergence. The results were compared with the numerical simulation data of Huang et al. [20] and the experimental values of Critzos et al. [36]

Table 2. Main mesh features and y-plus peak values at a Reynolds number of 5×10^5 and an angle of attack of 10°.

Number of cells	First row	Growth factor	Peak Y-plus value
8096	5×10^{-3}	1.1	105
17160	1×10^{-3}	1.1	25
24480	2×10^{-4}	1.1	5.52
40640	1×10^{-4}	1.1	1.60
58080	1×10^{-5}	1.1	0.45

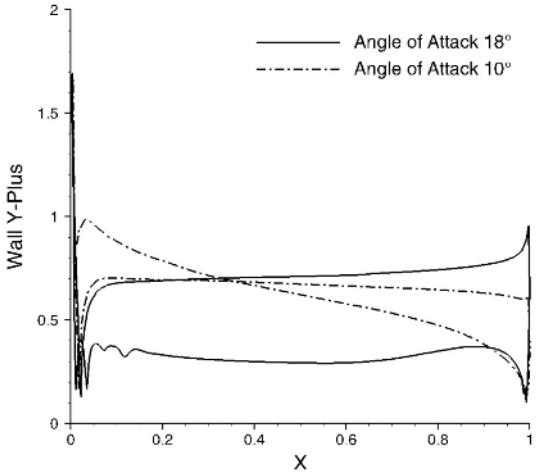

Fig. 3. Wall y-plus distribution over the NACA 0012 airfoil at angles of attack of 10 and 18°.

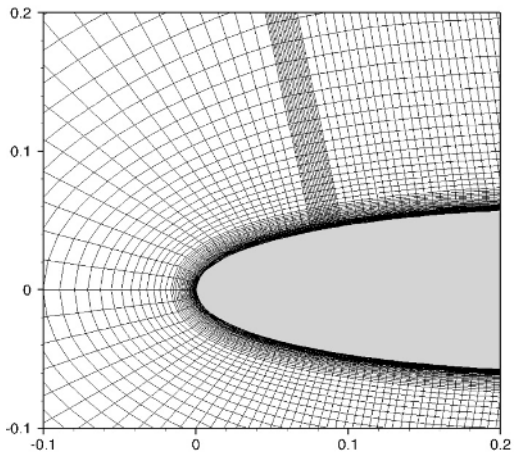

Fig. 4. Structured grid of NACA 0012 airfoil with jet slot.

and Jacobs et al. [37]. Huang et al. investigated the suction and blowing flow control over a NACA 0012 airfoil under a Reynolds number of 5×10^5 and an angle of attack of 18°. Moreover, they examined several parameters, including jet location, jet amplitude, and jet angle, through the CFD GHOST code. Critzos et al. experimentally studied the aerodynamic characteristics of a NACA 0012 airfoil, with Reynolds numbers of 0.5×10^6 and 1.8×10^6 and angles of attack varied from 0° to 180°. E. Jacobs et al. investigated symmetrical NACA airfoils in wind tunnel over a wide range of Rey-

Table 3. Comparison of computational lift coefficient and experimental values at angles of attack less than 10°.

Angle of attack	Computational results	Experimental result of Critzos et al. [36]	Experimental result of Jacobs et al. [37]	Experimental result of Sheldahl et al. [38]
0°	0.0021	0.0	0.0	0.0
2°	0.1853	0.2053	0.1807	0.22
5°	0.4715	0.5855	0.4511	0.55
10°	0.9087	0.9542	0.9019	1.003

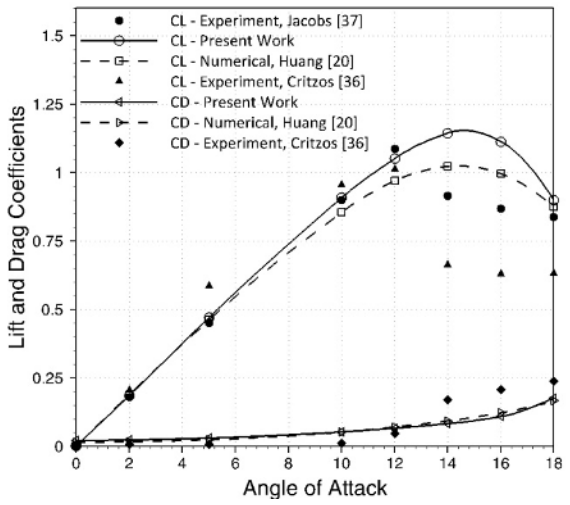

Fig. 5. Comparison among the current computational results, the numerical work result of Huang et al. [20], and the experimental measurement results of Critzos et al. [36] and Jacobs et al. [37].

Table 4. Comparison of computational results and numerical study [20] for blowing and suction flow control.

Case study	Perpendicular blowing		Tangential blowing		Suction	
	$\frac{C_L}{C_{L,Base}}$	$\frac{C_D}{C_{D,Base}}$	$\frac{C_L}{C_{L,Base}}$	$\frac{C_D}{C_{D,Base}}$	$\frac{C_L}{C_{L,Base}}$	$\frac{C_D}{C_{D,Base}}$
Huang et al. [20]	1.023	0.902	1.048	0.925	1.243	0.805
Present study	1.021	0.897	1.070	0.926	1.295	0.708

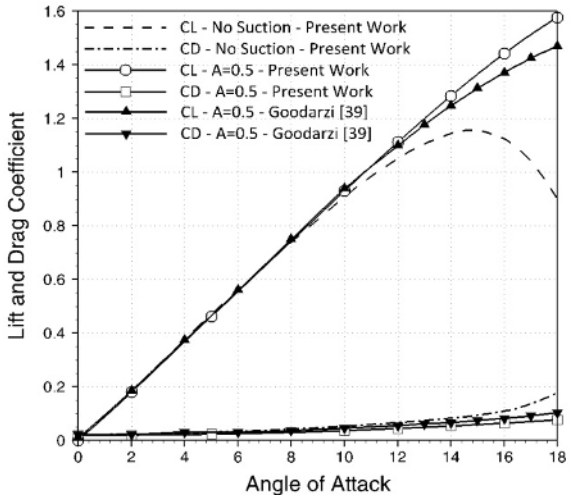

Fig. 6. Comparison of computational results and numerical study [39] for suction flow control.

nolds numbers. The results of the present work were compared with the above-mentioned studies in Fig. 5. The figure indicates that the current computation results show good agreement with the numerical simulation of Huang et al. and the experimental data of Jacobs et al. The current highest recorded error for lift and drag coefficients was 8% higher than that of Huang et al. and 15% higher than that of Jacobs et al. at an angle of attack 14°. The stall angle in both numerical works occurred at an angle of attack of 14°, while, the empirical measurements indicate that the NACA 0012 airfoil stall occurred at an angle of attack of 12°. The computational results of lift and drag coefficients show better agreement with experimental data than with other numerical studies until an angle of attack of 12°. The comparison of computational results at low angles of attack (less than 10°) with the experimental data [36-38] is provided in Table 3 (all experimental data have a Reynolds number of 5×10^5). Fig. 5 and Table 3 show that the experimental data from literature significantly varied, which implies a large amount of experimental uncertainty. This uncertainty is attributed to several factors, such as different flow regimes, angles of attack, and airfoil geometries.

Turbulence model selection has a significant effect on stall prediction and lift-to-drag ratio accuracy. The k-ε realizable model at the same condition, caused a stall angle of 16° instead of 14°, and theretofore, the k-ω ST model has better stall prediction capability. The k-ω SST model has better stall prediction capability than the k-ε realizable model. Moreover the prediction by k-ε realizable was good in the pre-stall region, but this model failed to predict the stall condition and post-stall phenomena accurately. The maximum errors for lift and drag coefficients in the k-ε realizable model at an angle of attack of 14° were 17% and 25%, respectively.

Given an apparent lack of experimental survey on suction and blowing flow control over a NACA 0012 airfoil at the current flow conditions, the computation results of airfoil with flow control were compared with numerical works. To validate the suction and blowing over NACA 0012 airfoil, the simulation data were compared with the numerical study of Huang et al. [20] under a Reynolds number of 5×10^5 and a suction/blowing jet width of 2.5% of the chord length conditions. $C_L/C_{L,\,Base}$ and $C_D/C_{D,\,Base}$ ratios were compared for the present study and [20] at a jet amplitude of 0.1 and an angle of attack of 18°, as shown in Table 4. In the study of Huang et al., the blowing and suction slots were located at 0.8 and 0.1 from the leading edge, respectively. Fig. 6 illustrates the comparison between the present study and the numerical work of Goodarzi et al. [39] under a Reynolds number of 5×10^5, a jet width of 2.5% of the chord length, a jet location of 10% of the

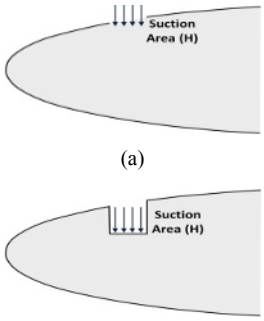

Fig. 7. Suction slot geometries for perpendicular suction over NACA 0012 airfoil: (a) type 1; (b) type 2.

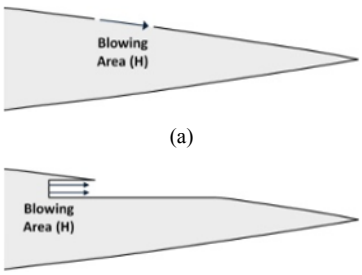

Fig. 8. Blowing slot geometries for tangential blowing over NACA 0012 airfoil: (a) type 1; (b) type 2.

chord length from the leading edge, and a jet amplitude of 0.5 at different angles of attack. The simulation results agree strongly with the mentioned studies.

3.3 Slot geometry

Two slot geometries are available for blowing and suction simulations over a NACA 0012 airfoil; their slot types are shown in Figs. 7 and 8. Due to the normal inlet and outlet flow directions, the perpendicular suction and perpendicular blowing have similar results, and so the result of perpendicular suction was used for perpendicular blowing. The streamlines and results of these two slot types were compared in Fig. 9 and Table 5. The perpendicular suction has a jet amplitude of 0.5, a jet width of 2.5% of the chord length, and angles of attack of 16 and 18°. The flow pattern around the airfoil for both suction slot geometry types is closely resembled. In experimental investigations, the slot geometry of type 1 for suction can be constructed through porous media. This type of geometry is also widely used in previous studies. In the current study, we also used slot geometry of type 1 for perpendicular suction and perpendicular blowing.

The comparison of streamlines around the airfoil and blowing slot for tangential blowing at the trailing edge is shown in Fig. 10. The values of lift and drag coefficients are presented in Table 6, which indicates that the results for two slot geometry types are strongly closed, whereas the vortexes passing the

Table 5. Comparison of lift and drag coefficients for different suction slot geometries.

Angle of attack	Suction slot geometry of type 1		Suction slot geometry of type 2	
	C_L	C_D	C_L	C_D
12°	1.1124	0.04474	1.1008	0.07025
14°	1.2846	0.05414	1.2707	0.08271
16°	1.4424	0.06487	1.4298	0.09193
18°	1.5778	0.07713	1.5605	0.10533

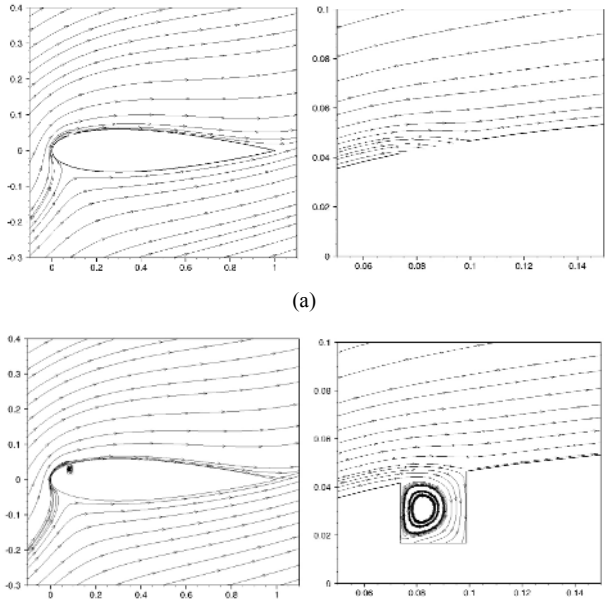

Fig. 9. Streamlines around the airfoil with a jet amplitude of 0.5, a jet width of 2.5%C, and an angle of attack of 18°: (a) suction slot geometry of type 1; (b) suction slot geometry of type 2.

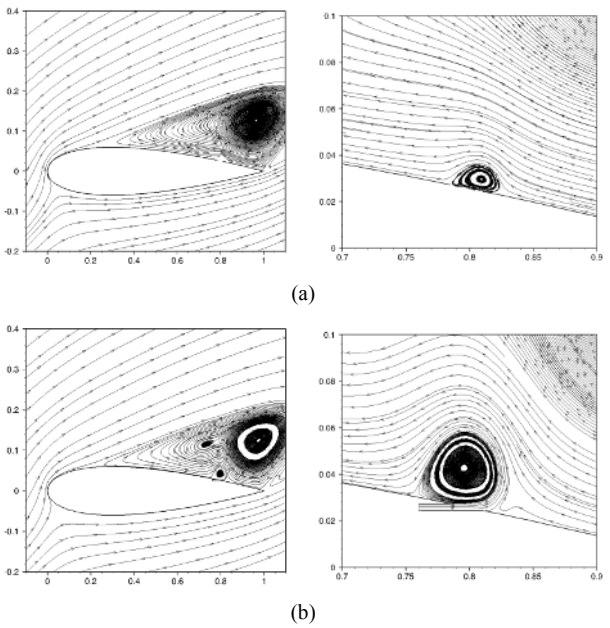

Fig. 10. Streamlines around the airfoil with a jet amplitude of 0.5, a jet width of 2.5%C, and an angle of attack of 18°: (a) blowing slot geometry of type 1; (b) blowing slot geometry of type 2.

Table 6. Comparison of lift and drag coefficients for different suction slot geometries.

Angle of attack	Blowing slot geometry of type 1		Blowing slot geometry of type 2	
	C_L	C_D	C_L	C_D
12°	1.0551	0.06994	1.0217	0.06918
14°	1.1596	0.08685	1.1388	0.08635
16°	1.1548	0.11015	1.1525	0.11074
18°	0.9659	0.16387	0.9749	0.16673

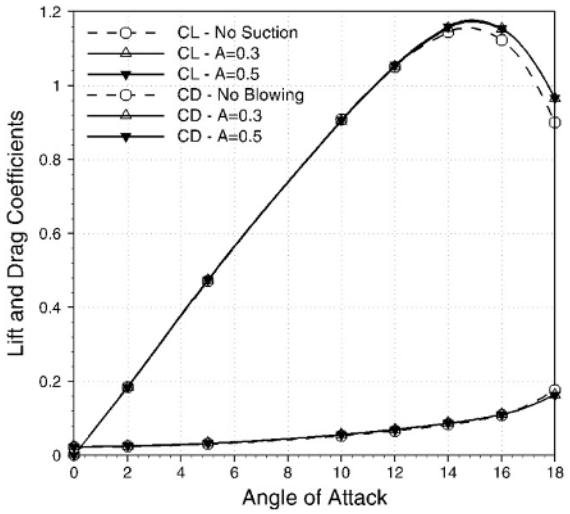

Fig. 11. Effects of blowing amplitude on lift and drag coefficients for tangential blowing at the airfoil trailing edge.

airfoil are different. The slot geometry of type 1 models the moving surface (wall motion) over the airfoils [40, 41] rather than the tangential blowing. Blowing is defined as a method of preventing separation to supply additional energy to the particles of fluid being retarded in the boundary layer [3]. The set up of slot geometry of type 1 in experimental surveys is roughly unreachable, whereas the slot geometry of type 2 is a common approach. Therefore, the blowing slot geometry of type 2 was used in this investigation for tangential blowing at the airfoil trailing edge.

4. Results and discussion

4.1 Tangential blowing

The effects of jet amplitude and jet width on lift and drag coefficients were investigated for tangential steady blowing at the trailing edge. The effects of blowing and its strength on aerodynamic coefficients are illustrated in Fig. 11 under conditions of L_j = 0.1C, H = 3.5%, and A = 0.3, 0.5. The figure indicates that the changes of jet amplitude have negligible effect on the aerodynamic characteristics of airfoil. The lift and drag coefficients are roughly constant with varying jet amplitude from 0.3 to 0.5. By applying blowing, lift coefficient increases progressively and drag coefficient decreases marginally. The maximum increase of lift-to-drag ratio occurred in a blowing amplitude of 0.5, which increased at approximately 16% at an angle of attack of 18°. The lift and drag coefficients had a 7% increase and decrease, respectively. When blowing amplitude increases, stall shows no alteration and occurs at the same angle of attack of 14°.

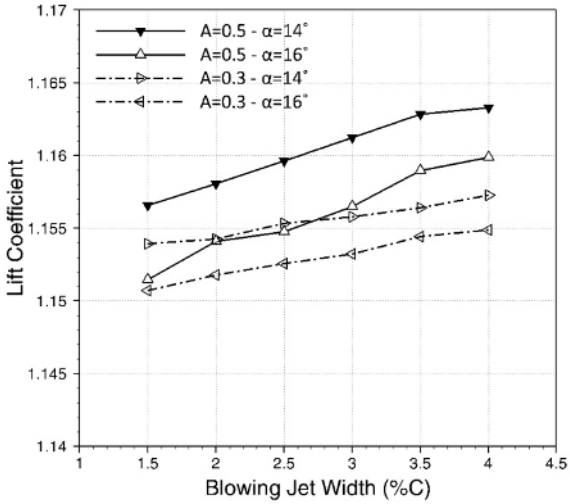

Fig. 12. Changes of lift coefficient with blowing jet width for jet amplitudes of 0.3 and 0.5 for tangential blowing at the trailing edge.

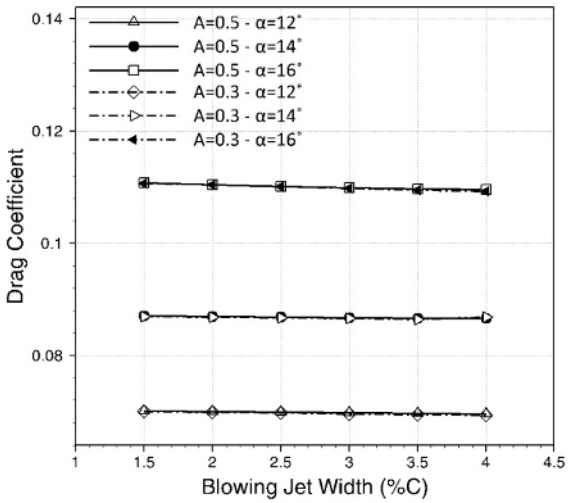

Fig. 13. Changes of drag coefficient with blowing jet width for jet amplitudes of 0.3 and 0.5 for tangential blowing at the trailing edge.

Figs. 12-14 present the lift, drag, and lift-to-drag ratio versus jet width with blowing jet amplitudes of 0.3 and 0.5 for tangential blowing at the trailing edge, respectively. Increasing the jet width leads to lift coefficient improvement and drag coefficient reduction slightly. Under an angle of attack of 14° and a blowing amplitude of 0.5, the lift coefficient increased to 1.157 and 1.163 for blowing jet widths of 1.5% and 4.0% of the chord length, respectively. Therefore, the lift coefficient increased approximately by 1%, whereas the drag coefficient remained nearly constant. The least improvement of the lift coefficient arises in jet widths of 3.5% to 4%, and the lift coef-

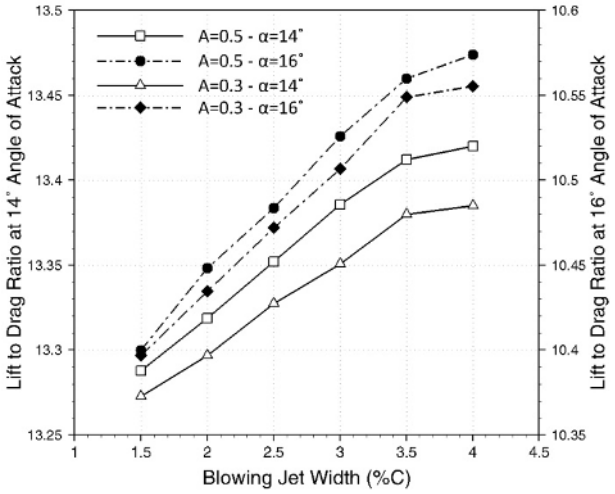

Fig. 14. Changes of lift-to-drag ratio with blowing jet width for jet amplitudes of 0.3 and 0.5 for tangential blowing at the trailing edge.

ficient value generally increases with a constant slope until a jet width of 3.5% of the chord length and then declines steadily. A similar trend was also found for the lift-to-drag ratio. By contrast, the drag coefficient reduces linearly as jet width increases. Moreover, the drag coefficient remains roughly constant in different jet amplitudes. In the conducted studies on tangential blowing, no maximum or minimum values were found in lift, drag, and lift-to-drag ratio. The vortexes around the blowing slot move toward downstream because of the tangential blowing at the airfoil trailing edge. Considerable vortexes are transferred to downstream by increasing the blowing jet width, as shown in Fig. 15.

The lift-to-drag ratio increases continually up to jet widths of 3.5% to 4% of the chord length along with jet width and then decreases. Hence, the blowing jet widths of 3.5% to 4% of the chord length are extremely effective. Generally, the variations of tangential blowing parameters have a remarkable effect on the lift coefficient and a marginal effect on the drag coefficient. As mentioned earlier, the blowing jet amplitude has an insignificant effect on aerodynamic coefficients and poses only a 2% increase in the lift-to-drag ratio. Consequently, the lift-to-drag ratio increased by 17% under a jet amplitude of 0.5, a jet width of 4% of the chord length, and an angle of attack of 18°. The streamline patterns of different jet widths passing an airfoil are plotted in Fig. 15 at a jet amplitude of 0.5 and an angle of attack of 16°. The streamlines when jet widths are 3.5% and 4% clearly demonstrate smaller vortex around the airfoil particularly closed to the blowing slot than other cases.

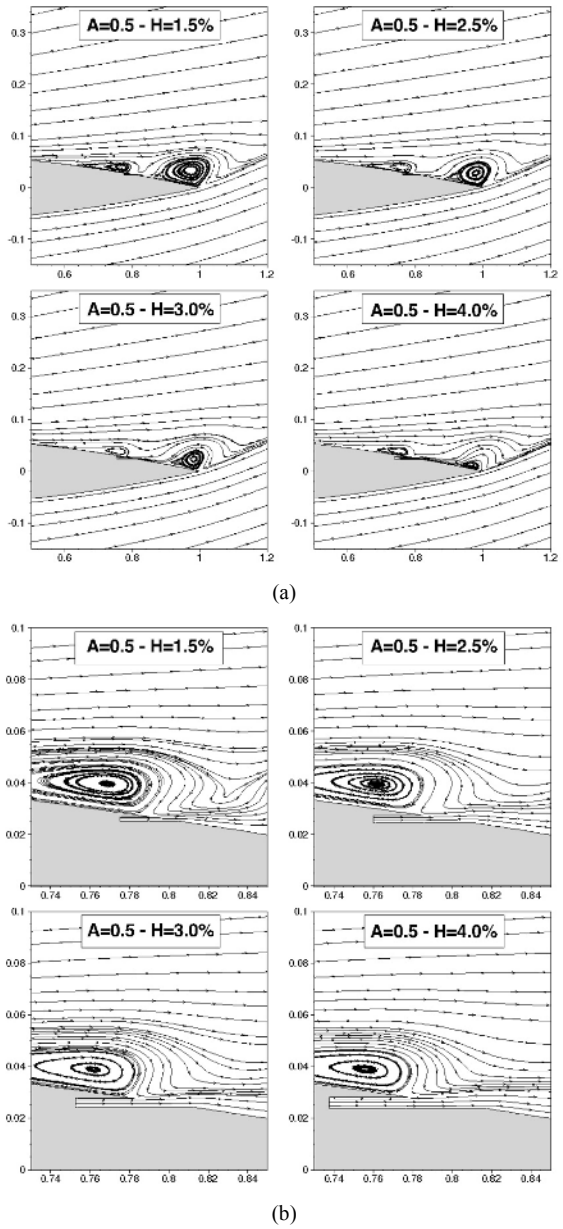

Fig. 15. Effects of blowing jet width on the vortexes around the (a) airfoil; (b) blowing slot at an angle of attack of 16° for tangential blowing.

4.2 Perpendicular blowing

Fig. 16 mainly focuses on the effects of jet amplitude variations with angle of attack for perpendicular blowing. In this subsection, the jet location was fixed at 0.8C, the jet width was considered as 1.5%C, the jet amplitude was limited to 0.3 and 0.5, and the jet angle was +90°. Smaller jet amplitude is more appropriate in perpendicular blowing, contrary to tangential blowing. The drag coefficient increased by approximately 8% and 5% for jet amplitudes of 0.3 and 0.5, respectively, at an angle of attack of 14°. On the contrary, the lift coefficient declined by approximately 8.5% and 14.5%. Generally, perpendicular blowing decreases the lift-to-drag ratio before stall angle intensively and increases the aerodynamic characteristics after stall, for instance, perpendicular blowing increased the lift-to-drag ratio by 17.5% at an angle of attack of 18°. Drag is usually an undesirable effect, and we do our

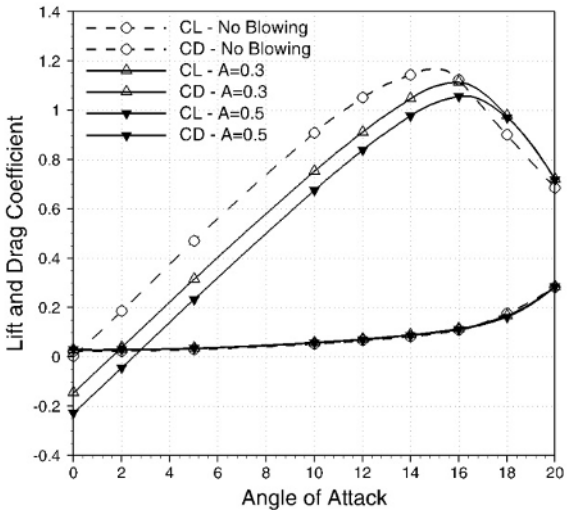

Fig. 16. Effects of blowing amplitude on lift and drag coefficients for perpendicular blowing at the trilling edge.

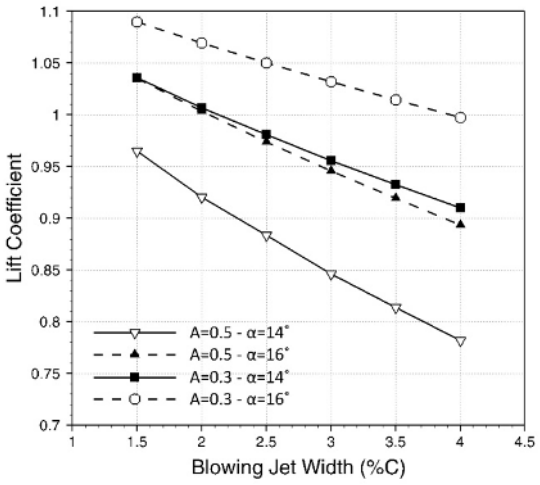

Fig. 17. Changes of lift coefficient with blowing jet width for jet amplitudes of 0.3 and 0.5 for perpendicular blowing at the trailing edge.

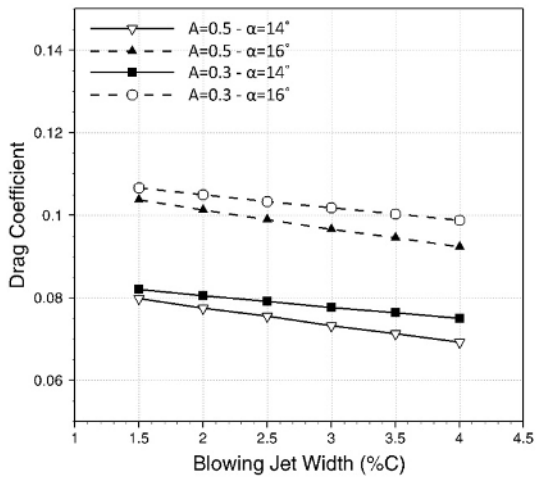

Fig. 18. Changes of drag coefficient with blowing jet width for jet amplitudes of 0.3 and 0.5 for perpendicular blowing at the trailing edge.

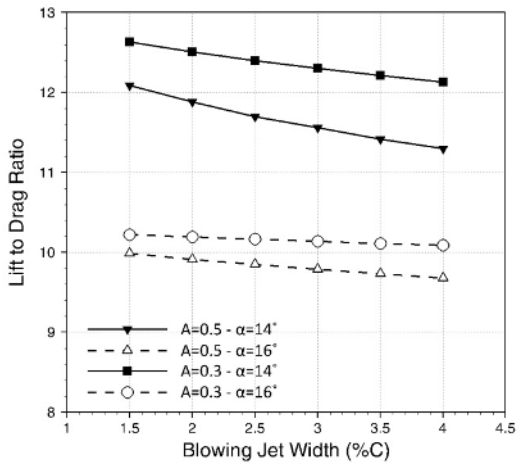

Fig. 19. Changes of lift-to-drag ratio with blowing jet width for jet amplitudes of 0.3 and 0.5 for perpendicular blowing at the trailing edge.

best to minimize it. The reduction of drag is closely associated with the reduction of fuel consumption, noise, and vibration. However, drag produces a beneficial effect in some cases, which we try to maximize, for example, in the brakes of airplanes.

Figs. 17-19 illustrate the changes of lift coefficient, drag coefficient, and lift-to-drag ratio with jet width and jet amplitude for perpendicular blowing at the airfoil trailing edge, respectively. Unlike in tangential blowing, the aerodynamic coefficients decrease continuously as blowing jet width increases in perpendicular blowing. When the jet width varied from 1.5% to 4% of the chord length, the lift and drag coefficients decreased by approximately 23% and 16%, respectively, under A = 0.5 and an angle of attack of 14°. In the similar conditions, the lift-to-drag ratio decreased by 7% and 3.5% at angles of attack of 14° and 16°, respectively. In all studied cases for perpendicular blowing, the decrease of lift and drag coefficients is almost linear with a constant slope. In Fig. 20, streamlines passing an airfoil for tangential and perpendicular blowing were compared at a blowing amplitude of 0.5 and an angle of attack of 16°. The perpendicular blowing in the trailing edge makes larger vortexes in comparison with tangential blowing. In addition, the velocity vectors over the airfoil surface were compared for tangential and perpendicular blowing, as shown in Fig. 21. The velocity vectors were plotted under a blowing jet width of 4% of the chord length, a blowing amplitude of 0.5, and an angle of attack of 16°. The tangential blowing postpones separation more than perpendicular blowing. The separation in tangential blowing occurred in 0.535 of the chord length, whereas that in perpendicular blowing occurred in 0.460 of the chord length from the airfoil leading edge. Consequently, we indicate that smaller blowing jet widths provide more positive effects for using perpendicular blowing to minimize drag and larger jet widths are effective to maximize it.

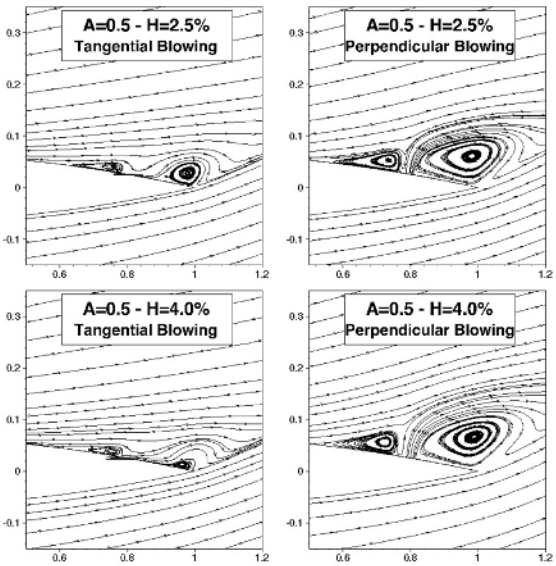

Fig. 20. Comparison between tangential and perpendicular blowing at a jet amplitude of 0.5, an angle of attack of 16°, and jet widths of 2.5 %C and 4 %C.

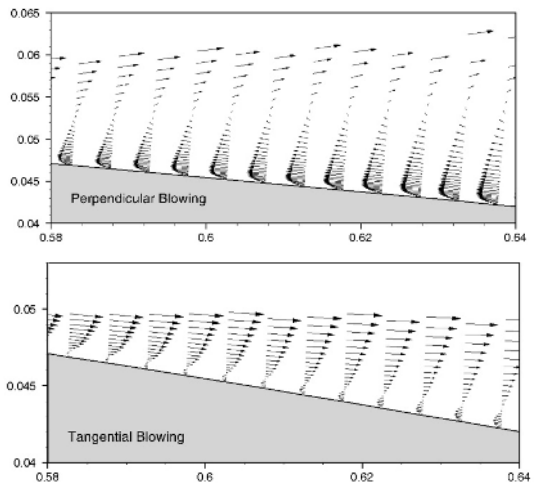

Fig. 21. Comparison between the velocity vectors of tangential and perpendicular uniform blowing, with a jet width of 4 %C, a blowing amplitude of 0.5, and an angle of attack of 16°.

4.3 Suction

The effects caused by the changes of suction amplitude were investigated in Fig. 22. The jet width and jet location were fixed at 2.5% and 10% of the chord length, respectively. As suction amplitude increased from 0.3 to 0.5, the lift coefficient improved and the drag coefficient declined. However, the lift coefficient increase and the drag coefficient decrease are negligible for angles of attack smaller than 10°. The lift coefficient increased by 75%, and the drag coefficient decreased by 56%, with a suction amplitude of 0.5 at an angle of attack of 18°. Moreover, increasing suction jet amplitude leads to stall angle improvement, which increased from 14° to 22° for jet

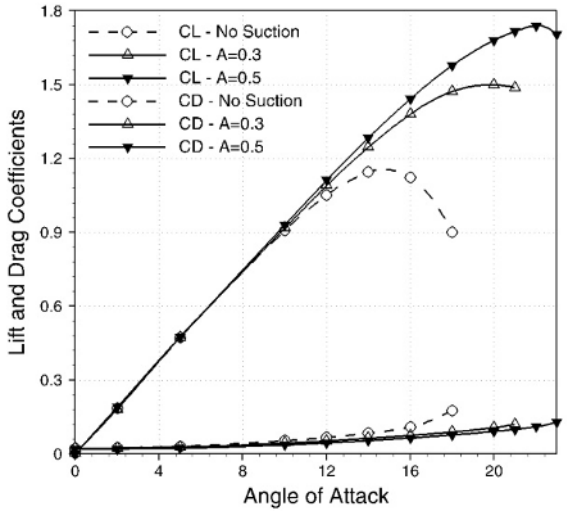

Fig. 22. Effects of suction amplitude on lift and drag coefficients for perpendicular suction.

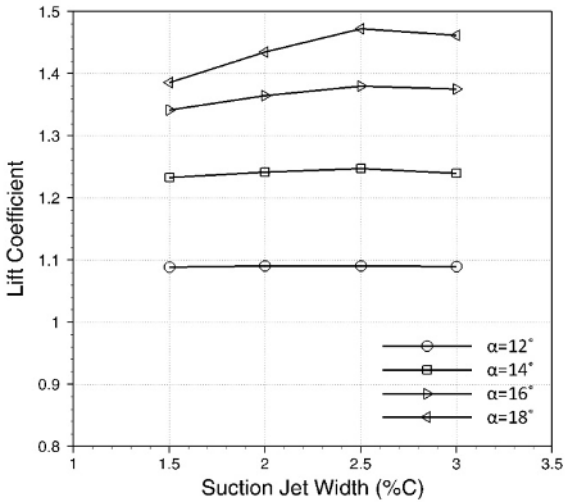

Fig. 23. Changes of lift coefficient with suction jet width for a jet amplitude of 0.3 for perpendicular suction at the leading edge.

amplitudes of 0 and 0.5, respectively. A jet amplitude of 0 refers to no suction conditions. With the use of perpendicular suction, not only the lift-to-drag ratio increases dramatically but also the stall angle delays effectively.

Figs. 23-25 show the lift, drag, and lift-to-drag ratio at different jet widths and angles of attack for perpendicular suction at the leading edge with a jet amplitude of 0.3, respectively. The variations in lift and drag coefficients with jet width are almost negligible at low angles of attack, although they have shown significant changes with the increment of angle of attack. With increasing jet width, the lift coefficient increases continuously until a jet width of 2.5% of the chord length and then insignificantly decreases. The drag coefficient has the similar trend. The lift coefficient increased by 6.3% and the drag coefficient reduced by 15% when the jet width varied from 1.5% to 2.5% of the chord length at an angle of attack of

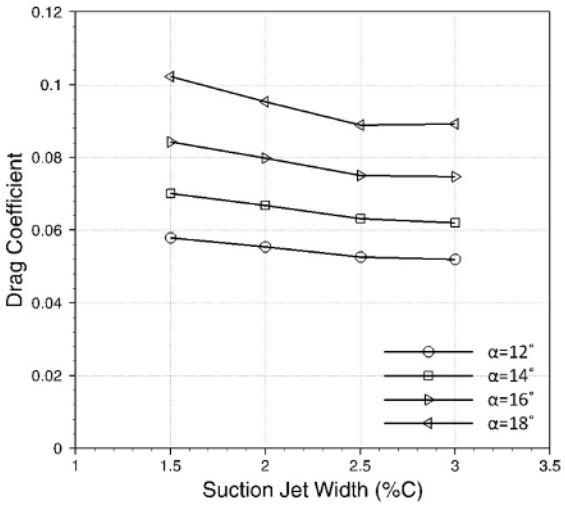

Fig. 24. Changes of drag coefficient with suction jet width for a jet amplitude of 0.3 for perpendicular suction at the leading edge.

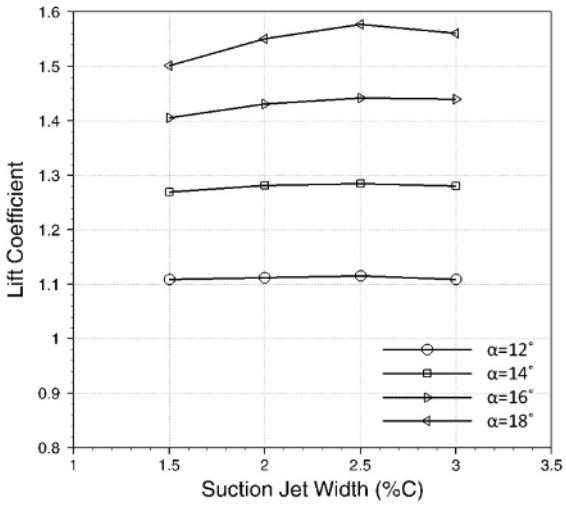

Fig. 26. Changes of lift coefficient with suction jet width for a jet amplitude of 0.5 for perpendicular suction at the leading edge.

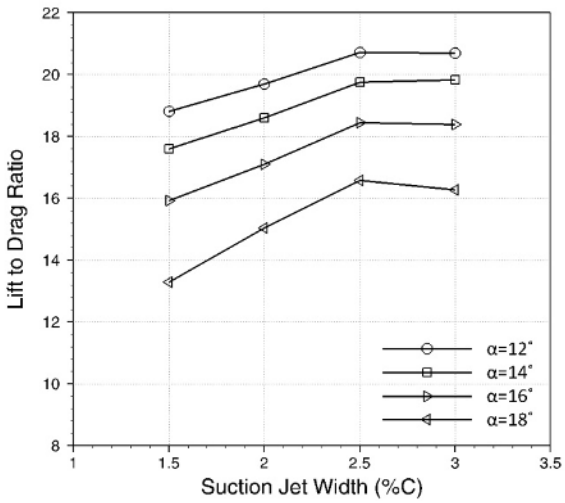

Fig. 25. Changes of lift-to-drag ratio with suction jet width for a jet amplitude of 0.3 for perpendicular suction at the leading edge.

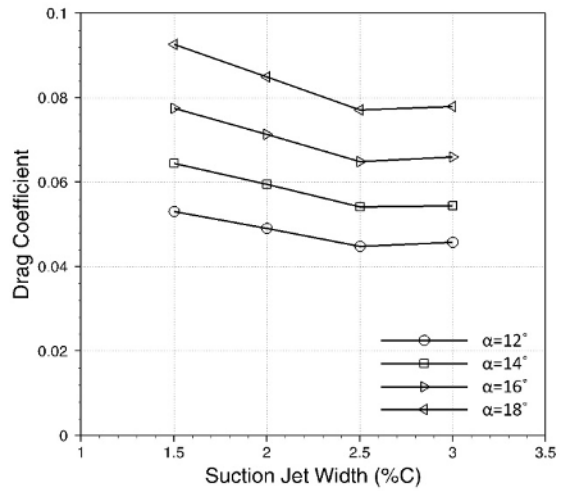

Fig. 27. Changes of drag coefficient with suction jet width for a jet amplitude of 0.5 for perpendicular suction at the leading edge.

18°. The jet width then increased from 2.5% to 3% of chord length, leading to trivial changes in the lift and drag coefficients. The lift-to-drag ratio also conforms to the above-mentioned trend and increased by 24% for jet width variation from 1.5% to 2.5%, whereas the lift-to-drag ratio increased only by 2% for jet width variation from 2.5% to 3% of chord length. Thus, the optimum jet width considered was 2.5% of the chord length for perpendicular suction at the leading edge.

Danenberg and Weiberg [7] experimentally evaluated the effects of suction jet width on a symmetrical airfoil (NACA airfoil 0010.51). They considered two slot widths, 2.3% and 6.3% of the chord length, for suction on the upper surface of airfoil and demonstrated that the optimum suction jet width was 2.3% of the chord length. The maximum lift increased approximately from 1.3 to 1.8 by an area suction of 2.3% of the chord length. The results of Ref. [7] confirm the obtained data of the present investigation.

Figs. 26-28 present the effects of suction jet amplitude, which changes from 0.3 to 0.5 for perpendicular suction at the airfoil leading edge. The lift coefficient increases until a jet width of 2.5% and then declines slightly particularly at high angles of attack. Increasing suction jet amplitude from 0.3 to 0.5 increases lift coefficient and reduces drag coefficient. The jet width increase from 2.5% to 3% led to a 1.4% reduction in the lift coefficient, a 1% improvement in the drag coefficient, and a 2.5% increase in the lift-to-drag ratio at angle of attack of 18°. In this case, the alterations of lift, drag, and lift-to-drag ratio were marginal at lower angles of attack.

Suction control on changing flow patterns at different jet widths is illustrated in Fig. 29. The results for suction jet widths of 1.5%, 2%, 2.5%, and 3% of the chord length are plotted and compared in the figure. These cases all have a jet

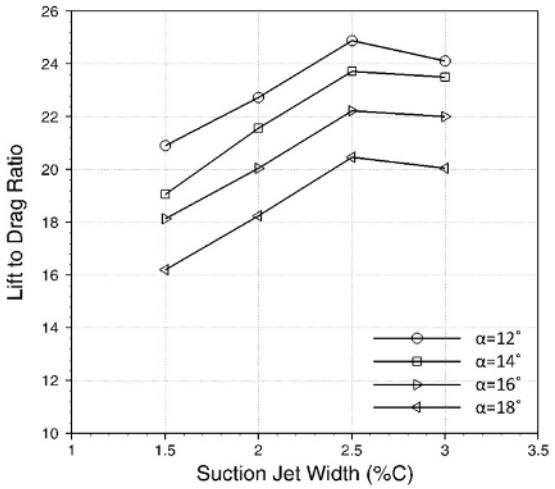

Fig. 28. Changes of lift-to-drag ratio with suction jet width for a jet amplitude of 0.5 for perpendicular suction at the leading edge.

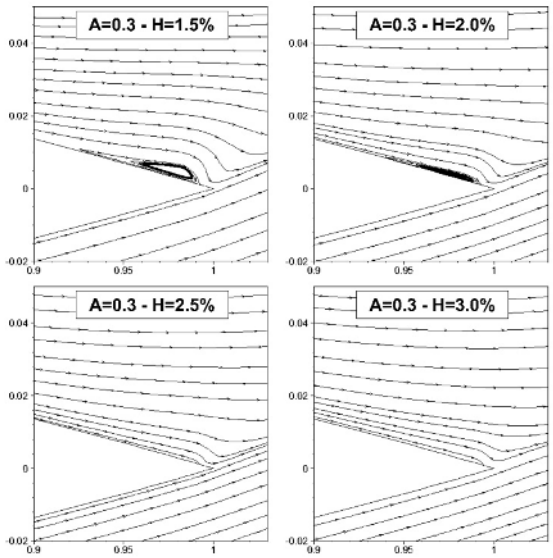

Fig. 29. Effect of suction jet width on eddies behind the airfoil at 16° angle of attack.

location of 10% of the chord length from the leading edge, a jet amplitude of 0.3 for perpendicular suction, and θ = −90°. When the jet width is increased, the separation bubble is effectively delayed; hence, the separation bubbles and vortices are almost entirely eliminated in a jet width of 2.5% of the chord length. Therefore, a suction jet width of approximately 2.5% to 3% of the chord length is the most effective width for the suction flow control approach to manipulate the boundary layer and increase the lift-to-drag ratio. An increase of suction area beyond of 3% of the chord length will not increase the aerodynamic characteristics significantly.

5. Conclusion

In this study, we evaluated the effects of blowing and suction flow controls on a NACA 0012 airfoil at a Reynolds number of 5×10^5, and different angles of attack. When a number of parameters, including jet width, jet amplitude, and jet angle, were changed and analyzed over a wide range, the following interesting and valuable results were obtained.

The computational studies were conducted with the blowing flow control approach. Downstream tangential blowing improves the lift and drag characteristics, whereas perpendicular blowing has often adverse effects in comparison with the desirable objectives of flow control results, particularly at angles of attack smaller than stall angle. However, smaller amplitudes are better than larger amplitudes for perpendicular blowing. The lift and drag coefficients are almost constant with variations of jet amplitude for tangential blowing. From a jet width standpoint increasing blowing jet width improves the lift-to-drag ratio continuously for tangential blowing and reduces it constantly and quasi-linearly for perpendicular blowing. The gradient of the lift-to-drag ratio declines from a jet width of 3.5% of the chord length in tangential blowing. Jet widths of 3.5% and 4% of the chord length appear to be the most effective choice for tangential blowing at the airfoil trailing edge. However, smaller jet widths pose more beneficial effects of using perpendicular blowing to minimize drag, whereas larger jet widths are highly efficient in maximizing drag. The lift-to-drag ratio increased by approximately 17% for tangential blowing under H = 4%, A = 0.5, and Lj = 0.8C from the leading edge, with an angle of attack of 18°.

The effects of suction control flow on the aerodynamic characteristics of NACA 0012 airfoil were subsequently investigated. In suction, larger amplitude results in larger effect on the flow field around the airfoil, particularly at high angles of attack. Owing to the use of perpendicular suction, not only the lift-to-drag ratio increases dramatically but also the stall angle improves effectively from 14° to 22°. From a jet width perspective the suction jet width improvement leads to a significant augmentation in the lift-to-drag ratio, and separation effectively travels toward downstream. The lift-to-drag ratio increases continuously until a jet width of 2.5% of the chord length and then decreases. By employing the suction control flow technique, the lift coefficient increased by approximately 75% and the drag coefficient decreased by 56% under H = 2.5%, A = 0.5, and Lj = 0.1C from the leading edge, with an angle of attack of 18°. The most effective jet widths for achieving all desirable effects are 2.5% to 3% of the chord length for suction at the airfoil leading edge.

Nomenclature

A : Jet amplitude
C : Airfoil chord length
C_μ : Momentum coefficient
H : Non-dimensional jet width
h : Jet width
k : Average kinetic energy
L_j : Jet location

P : Pressure
u : X-axis direction velocity
u_j : Jet velocity
u_∞ : Free-stream velocity
v : Y-axis direction velocity
α : Angle of attack
β : Angle between free-stream velocity direction and the local jet surface
δ_{ij} : Kronecker delta
θ : Angle between the local jet surface and jet exit velocity direction
ν : Kinetic viscosity
ν_t : Turbulent viscosity
ρ : Density

References

[1] D. C. Hazen, Boundary layer control, *Journal of Fluid Mechanics*, 29 (1968) 200-208.

[2] M. Gad-el-hak, *Control flow: Passive, active and reactive flow management*, Cambridge University Press, United Kingdom (2000) 25-35.

[3] H. Schlichting, *Boundary layer theory*, McGraw-Hill, New York, USA (1968) 347-362.

[4] E. J. Richards and C. H. Burge, *An airfoil designed to give laminar flow over the surface with boundary layer suction*, Aeronautical Research Council, R&M 2263 (1943).

[5] S. W. Walker and W. G. Raymer, *Wind tunnel test on the 30 percent symmetrical griffth aerofoil with ejection of air*, Aeronautical Research Council, R&M 2475 (1946).

[6] A. L. Braslow, *A history of suction type laminar flow control with emphasis on flight research*, NASA History Division, Monograph in Aerospace History, 13 (1999).

[7] R. E Dannenberg and J. A. Weiberg, Section characteristics of a 10.5 percent thick airfoil with area suction as affected by chordwise distribution of permeability, *NACA Technical Note 2847* (1952).

[8] D. M. Heugen, An experimental study of a symmetrical aerofoil with a rear suction slot and a retractable flap, *Journal of Royal Aeronautical Society*, 57 (1953).

[9] R. E. Dannenberg and J. A. Weiberg, Section characteristics of an NACA0006 airfoil with area suction near the leading edge, *NACA Technical Note 3285* (1954).

[10] H. J. Howe and B. J. Neumann, *An experimental evaluation of a low propulsive power discrete suction concept applied to an axisymmetric vehicle*, David W. Taylor Naval Ship R&D Center TM 16-82/02 (1982).

[11] S. Dirlik, K. Kimmel, A. Sekelsky and J. Slomski, Experimental evaluation of a 50-percent thick airfoil with blowing and suction boundary layer control, *AIAA Paper No. AIAA-92-4500* (1992).

[12] Y. Guowei, W. Shanwu, L. Ningyu and Z. Lixian, Control of unsteady vertical lift on an airfoil by leading-edge blowing suction, *ACTA Mechanica Sinica (English Series)*, 13 (4) (1997) 304-312.

[13] J. Z. Wu, X. Y. Lu, A. G. Denny, M. Fan and J. M. Wu, Post-stall flow control on an airfoil by local unsteady forcing, *Journal of Fluid Mechanics*, 371 (1998) 21-58.

[14] C. Nae, Synthetics jets influence on NACA0012 airfoil at high angle of attacks, *AIAA Paper No. AIAA-98-4523* (1998).

[15] S. S. Ravindran, Active control of flow separation over an airfoil, *Report of Langley Research Center* (1999).

[16] D. P. Rizzetta, M. R. Visbal and M. J. Stank, Numerical investigation of synthetic jet flow fields, *AIAA Journal*, 37 (8) (1999) 919-927.

[17] M. B. Glauert, The application of the exact method of aerofoil design, Aeronautical Research Council, *R&M 2683* (1947).

[18] J. H. Preston, N. Gregory and A. G. Rawcliffe, The theoretical estimation of power requirements for slot-suction aerofoils with numerical results for two thick griffith type sections, Aeronautical Research Council, *R&M 1577* (1948).

[19] D. F. Abzalilov, L. A. Aksentev and N. B. IL'Inskii, The inverse boundary-value problem for an airfoil with a suction slot, *Journal of Applied Mathematics and Mechanics*, 61 (1) (1997) 75-82.

[20] L. Huang, P. G. Huang and R. P. LeBeau, Numerical study of blowing and suction control mechanism on NACA0012 airfoil, *Journal of Aircraft*, 41 (5) (2004) 1005-1013.

[21] C. R. Rosas, Numerical simulation of flow separation control by oscillatort fluid injection, *Doctor of Philosophy Thesis*, A&M University, Texas (2005).

[22] N. K. Beliganur and P. Raymond, Application of evolutionary algorithms to flow control optimization, *Report of University of Kentuchky* (2007).

[23] E. Akcayoz and I. H. Tuncer, *Numerical investigation of flow control over an airfoil using synthetic jets and its optimization*, International Aerospace Conference, Turkey (2009).

[24] C. Jensch, K. C. Pfingsten and R. Radespiel, Numerical investigation of leading edge blowing and optimization of the slot geometry for a circulation control airfoil, *Notes on Numerical Fluid Mechanics and Multidisciplinary Design*, 112 (2010) 183-190.

[25] D. You and P. Moin, Active control of flow separation over an airfoil using synthetic jets, *Journal of Fluids and Structures*, 24 (8) (2008) 1349-1357.

[26] S. H. Kim and C. Kim, Separation control on NACA23012 using synthetic jet, *Aerospace Science and Technology*, 13 (4) (2009) 172-182.

[27] M. S. Genc, U. Keynak and H. Yapici, Performance of transition model for predicting low re aerofoil flows without/with single and simultaneous blowing and suction, *European Journal of Mechanics B/Fluids*, 30 (2) (2011) 218-235.

[28] C. L. Rumsey and T. Nishino, Numerical study comparing RANS and LES approaches on a circulation control airfoil, *International Journal of Heat and Fluid Flow*, 32 (5) (2011) 847-864.

[29] T. Lee and Y. Y Su, Unsteady airfoil with a harmonically deflected trailing edge flap, *Journal of Fluids and Structures*,

27 (8) (2011) 1411-1424.
[30] E. Benini, R. Biollo and R. Ponza, Efficiency enhancement in transonic compressor rotor blades using synthetic jets: A numerical investigation, *Applied Energy*, 88 (3) (2011) 953-962.
[31] B. Yagiz, O. Kandil and Y. V. Pehlivanoglu, Drag minimization using active and passive flow control techniques, *Aerospace Science and Technology*, 17 (1) (2012) 21-31.
[32] K. Yousefi, S. R. Saleh and P. Zahedi, Numerical study of flow separation control by tangential and perpendicular blowing on the NACA 0012 airfoil, *International Journal of Engineering*, 7 (1) (2013) 10-24.
[33] K. Yousefi, S. R. Saleh and P. Zahedi, Numerical investigation of suction and length of suction jet on aerodynamic characteristics of the NACA 0012 airfoil, *International Journal of Materials, Mechanics and Manufacturing*, 1 (2) (2013) 136-142.
[34] G. Alfonsi, Reynolds-averaged Navier-Stokes equations for turbulence modeling, *Applied Mechanics Reviews*, 62 (4) (2009) 040802.
[35] F. R. Menter, M. Kuntz and R. Langtry, Ten years of industrial experience with the SST turbulence model, *Proceedings of 4th International Symposium on Turbulence, Heat and Mass Transfer*, Turkey (2003) 625-632.
[36] C. C. Critzos, H. H. Heyson and W. Boswinkle, Aerodynamics characteristics of NACA0012 airfoil section at angle of attacks from 0° to 180°, *NACA Technical Note 3361* (1955).
[37] E. Jacobs and A. Sherman, Airfoil section characteristics as affected by variations of the Reynolds number, *NACA Report No. 586-231* (1937).
[38] R. E. Sheldahl and Klimas, Aerodynamic characteristics of seven airfoil section through 180 degrees angle of attack for use in aerodynamic analysis of vertical axis wind turbines, Sandia National Labs., *Report No. SAND80-2114* (1981).
[39] M. Goodarzi, R. Fereidouni and M. Rahimi, Investigation of flow control over a NACA0012 airfoil by suction effect on aerodynamic characteristics, *Canadian Journal on Mechanical Sciences and Engineering*, 3 (3) (2012) 102-109.
[40] V. J. Modi, F. Mokhtarian and T. Yokomizo, Effects of moving surfaces on the airfoil boundary-layer control, *Journal of Aircraft*, 27 (1) (1990) 42-50.
[41] K. Yousefi, S. R. Saleh, P. Zahedi and Y. Noori, *Numerical investigation of moving surface boundary-layer control on NACA 0012 airfoil and comparison with tangential and perpendicular blowing*, 21th Annual International Conference on Mechanical Engineering (ISME), Tehran, Iran (2013).

Kianoosh Yousefi received his B.Sc. and M.Sc. degrees in Mechanical Engineering from Islamic Azad University, Mashhad Branch, Iran in 2009 and 2013, respectively, with great distinction. His research interests include aerodynamics, fluid mechanics, multiphase flows, and combustion. Mr. Yousefi's primary research focus is currently the active/passive flow control methods and turbulent flows.

S. Reza Saleh received his B.Sc. and M.Sc. degrees in Mechanical Engineering from Ferdowsi University, Iran in 1994 and 1997, respectively. He then received his Ph.D. in Mechanical Engineering - Energy conversion from Ferdowsi University, Iran in 2002. Dr. Saleh is currently an Assistant Professor of Mechanical Engineering Department at Islamic Azad University, Mashhad Branch, Iran. Dr. Saleh's research interests include computational fluid dynamics, similarity, and exact solution.

Peyman Zahedi received his M.Sc. degree in Mechanical Engineering in February 2013 from Islamic Azad University, Mashhad Branch, Iran. His research interests include combustion, multiphase flows, computational fluid dynamics, and flow control techniques.